HHS Public Access

Author manuscript

Oncogene. Author manuscript; available in PMC 2014 October 10.

Published in final edited form as:

Oncogene. 2014 April 10; 33(15): 2004–2010. doi:10.1038/onc.2013.149.

Siah2 regulates tight junction integrity and cell polarity through control of ASPP2 stability

Hyungsoo Kim[1], **Guisepinna Claps**[1], **Andreas Möller**[2], **David Bowtell**[2,3], **Xin Lu**[4], and **Ze'ev A. Ronai**[1]

[1]Signal Transduction Program, Cancer Center, Sanford-Burnham Medical Research Institute, La Jolla, CA, 92037 USA

[2]Research Division, Peter McCallum Cancer Centre, Melbourne 8006, VIC, Australia

[3]The Department of Biochemistry, University of Melbourne, Parkville 3010 Australia

[4]Ludwig Institute, Oxford, UK

Abstract

Changes in cell adhesion and polarity are closely associated with epithelial cell transformation and metastatic capacity. The tumor suppressor protein ASPP2 has been implicated in control of cell adhesion and polarity, through its effect on the PAR complex. Here we demonstrate that under hypoxic conditions the ubiquitin ligase Siah2 controls ASPP2 availability, with concomitant effect on epithelial cell polarity. LC-MS/MS analysis identified ASPP2 and ASPP1 as Siah2 interacting proteins. Biochemical analysis confirmed this interaction and mapped degron motifs within ASPP2, which are required for Siah2-mediated ubiquitination and proteasomal-dependent degradation. Inhibition of Siah2 expression increases ASPP2 levels and enhances ASPP2-dependent maintenance of TJ integrity and polarized architecture in 3D organotypic culture. Conversely, increase of Siah2 expression under hypoxia decreases ASPP2 levels and the formation of apical polarity in 3D culture. In all, our studies demonstrate the role of Siah2 in regulation of TJ integrity and cell polarity under hypoxia, through its regulation of ASPP2 stability.

Keywords

ASPP2; Siah2; epithelial polarity; tight junction; hypoxia

Introduction

The ubiquitin-proteasome system plays a fundamental role in the post-translational control of pathways engaged in normal and stress-altered homeostasis, and is thus intimately

Correspondence: Ze'ev A. Ronai, Signal Transduction Program, Sanford-Burnham Medical Research Institute, 10901 N Torrey Pines Rd, La Jolla, CA, 92037, USA. Tel, 858.646.3185; ronai@sbmri.org.

Conflict of interest: The authors declare that they have no conflict of interest.

involved in numerous pathophysiological processes. Members of the Siah (seven in absentia homolog) family are mammalian homologs of the *Drosophila* Sina (seven in absentia). Siah ubiquitin ligases contain RING domains and target growing number of substrates for ubiquitin-dependent proteasomal degradation.[1] In mammals, Siah1 and Siah2 are implicated in the control of several key cellular responses. Siah-dependent regulation of prolyl hydroxylases (PHDs), HIPK2 or AKAP121, for example, takes place primarily under hypoxic conditions and links Siah proteins to the control of hypoxia, DNA damage responses, and mitochondrial dynamics.[2-4] Siah plays a physiological role in Ras signaling that is conserved from *Drosophila* to mammals.[5, 6] An increasing number of studies, employing a variety of cancer models, have demonstrated the role of Siah proteins in tumor development and metastasis.[6-9]

Here, we identify ASPP1 and ASPP2, two of the three members of the ASPP (Apoptosis Stimulating Proteins of p53) family, as Siah-interacting proteins and substrates. ASPP proteins were shown to play a role in the transcriptional control of apoptosis-related genes, in part through their effect on p53 family proteins.[10, 11] Studies in the ASPP2-deficient mouse support a role for ASPP2 as a tumor suppressor.[12] Recent studies have pointed to a role for ASPP2 in the regulation of cell-cell adhesion and cell polarity. dASPP (*Drosophila* homolog of ASPP2) modulates cell-cell adhesion and ASPP2 and PAR-3 in mammalian cells regulate TJ formation in an interdependent manner.[13-15] Several mechanisms have been shown to control ASPP2, including epigenetic silencing, EF1-mediated transcription, and proteasome-dependent degradation.[16-19] Here, we identified Siah E3 ligases that control the stability of ASPP1 and ASPP2 proteins. By controlling the availability of ASPP2, Siah2 emerges as an important regulator of cell-cell junction integrity and cell polarity under hypoxia.

Results and discussion

Siah2 Interacts with ASPP1 and ASPP2

Search for putative new Siah2 substrates was performed using LC-MS/MS analysis of proteins bound to a ligase-deficient Siah2 RING mutant (Siah2RM). Among Siah2-bound proteins this analysis confirmed three known Siah-interacting proteins, OGDH (2-oxoglutarate dehydrogenase), GAPDH (glyceraldehyde-3-phosphate dehydrogenase), and TPX2 (microtubule-associated protein homolog) (supplementary Figure S1a).[20-22] Notably, this analysis also identified high number of peptides for two members of the ASPP proteins, ASPP1 and ASPP2. Initial support for the possibility that ASPPs may be Siah2 substrates was the finding that both proteins contained Siah2 degrons (supplementary Figure S1a) and that bands corresponding to the expected molecular weight of ASPP proteins were detected in the silver staining analysis of Siah2 interacting proteins (supplementary Figure S1b). These initial observations were corroborated by a series of Siah1/2-ASPP1/2 biochemical studies. First, we observed a specific interaction between ASPP1/2 and Siah1/2 using ectopically expressed proteins (Figure 1a; supplementary Figure S1c). Of interest, the *in vitro* analysis for ASPP1/2-Siah1/2 interaction was higher using immunoprecipitated ASPP1 and ASPP2, (Figure 1b; supplementary Figure S1d and S1e), suggesting that ASPP1/2 may be subject to post-translational modification required for efficient interaction with Siah2.

Notably, specific interaction between endogenous ASPP1/2 and Siah2 was also detected, albeit, in the presence of the proteasome inhibitor, implying that inhibition of proteasome-dependent degradation of ASPP1/2 upon association with Siah2 increases the available pool of ASPP1/2 for interacting with Siah2 (Figure 1c; supplementary Figure S1f). That input level of ASPP2 was not increased in cells treated with MG132 is consistent with the notion that ASPP2 requires post-translational modification for efficient recognition by Siah2, enriched upon IP. Among the two ubiquitin ligases, endogenous Siah2, but not Siah1, was found to interact with ASPPs, implying physiological relevant regulation of these substrates by Siah2.

ASPP2 Interaction with- and Degradation by- Siah2 is mediated by the Conserved Siah-Degrons

Expression of wild type (WT) Siah1 and Siah2 efficiently reduced the steady-state levels of ASPP1 and ASPP2, while the ligase-deficient RING mutant proteins did not elicit this change, suggesting Siah1/2 requires its ubiquitin ligase activity for regulation of ASPP1/2 protein stability (Figure 1d; supplementary Figure S2a and 2b). Common to Siah substrates is the presence of Siah degron (P×A×V×P or V×A×V×P), which is required for Siah2 interaction and concomitant ubiquitination-dependent degradation.[23] Given the presence of putative degrons in ASPP1 and ASPP2, we tested their possible requirement for Siah effect (supplementary Figure S2c). Deletion of both degrons (N341) abolished ASPP2-Siah2 interaction and significantly attenuated ASPP2 degradation by Siah2 (Figure 1e and 1f; supplementary Figure S2d). Consistent with this, mutation of the two degrons significantly attenuated ASPP2 degradation by Siah2 (Figure 1g), pointing to the requirement of these degrons for Siah2 control of ASPP2 stability.

ASPP1/2 stability is regulated by Siah2-dependent proteasomal degradation

To further establish the role of Siah2 in the control of ASPP1/2 protein stability, we analyzed S*iah1a*$^{+/+}$ *Siah2*$^{+/+}$ (WT) and *Siah1a*$^{-/-}$ *Siah2*$^{-/-}$ (DKO) mouse embryonic fibroblasts (MEFs).[4] In agreement with previous observations, the steady-state level of ASPP1 and ASPP2 proteins was higher in DKO than WT MEFs (Figure 2a). Notably, the level of iASPP, the third member of the ASPP family, which contains a homologous C-terminus but lacks the Siah-degron, was not altered in DKO cells (Figure 2a).[24] There was no corresponding increase of ASPP1 and ASPP2 transcripts in DKO cells (Figure 2b). Consistent with the changes seen at the protein level, Siah2 knockdown (KD) in WT MEFs increased the level of ASPP2 and ASPP1 proteins (Figure 2c). Furthermore, stable expression of Siah2RM in WT MEFs increased the steady state level of ASPP1 and ASPP2 protein, but not their transcripts (Figure 2e), suggesting that Siah2RM outcompetes endogenous Siah effect on ASPP2 stability.

We further examined the involvement of the proteasomes in Siah2-mediated control of ASPP expression. Inhibition of proteasome activity increased ASPP1 and ASPP2 expression in WT, but not in DKO MEFs (Figure 2d), supporting a role for Siah1/2 in proteasome-dependent regulation of ASPP1/2 stability.

We next analyzed the effect of Siah2 on the half-life of ASPP2. Under inhibition of protein synthesis the half-life of ASPP2 was significantly prolonged in DKO MEFs (Figure 2f). Consistent with these observations, high molecular weight forms of ASPP2 were evident in cells expressing Siah2 WT, which were further increased upon treatment with MG132 (Figure 2g), suggesting these are ubiquitin chains conjugated to ASPP2. Similarly, in vitro ubiquitination reactions using bacterially expressed Siah2, but not Siah2RM, efficiently caused the ubiquitination of immunopurified ASPP2. Collectively, these findings establish that ASPP1/2 are Siah1/2 substrates and that their stability is regulated by Siah-dependent ubiquitination and proteasome-dependent degradation.

Siah2 regulates TJ integrity by controlling ASPP2 expression

Given the growing evidence supporting a role for ASPP2 in control of TJ formation and cell polarity,[14, 15] we asked whether Siah2 regulation of ASPP2 stability would affect TJ. Consistent with previous reports, reduced expression of ASPP2 in NRK-52E, kidney tubular epithelial cells, significantly attenuated ZO-1 re-localization to TJ and impaired barrier function (lower TEER value) upon calcium recovery (Figure 3a-d; supplementary Figure S3a and S3b).[14, 15] Conversely, KD of Siah2 and overexpression of ASPP2 significantly accelerated TJ assembly as evidenced by a rapid re-localization of ZO-1 at cell junction and significantly enhanced barrier function (higher TEER value) compared to control (Figure 3a-d), pointing to the importance of Siah2-ASPP2 regulatory axis in TJ formation. Consistent with these observations is the finding that ectopically expressed Siah inhibitory peptide derived from the fly phyllopod protein (PHYL-130, consists of the N-terminus 130 amino acids from phyllopod protein in *D. melanoganster*),[25] efficiently attenuated the activity of endogenous Siah2 as reflected in stabilized ASPP2 protein and increased re-localization of ZO-1 at cell-cell contact. These findings substantiate the role of Siah2 in the regulation of TJ formation (Figure 3e; supplementary Figure S3c).

Given the disruption of cell-cell junction during epithelial-mesenchymal transition (EMT), we next explored a role for Siah2 and/or ASPP2 in TJ integrity during EMT.[26] For this we chose NMuMG cells, a classical model for studying TGF-β-driven EMT, and established stable clones expressing shRNA targeting Siah2, ASPP2, or both, or Siah2-resistant ASPP2, due to mutation within the Siah2 degrons (Figure 3f and 3g). TGF-β stimulation, required to achieve the EMT phenotype in these cells, reflected in disruption of TJ. Significantly, Siah2 KD markedly attenuated TGF-β ability to induce TJ disruption, monitored by ZO-1 localization at cell junction. Furthermore, KD of ASPP2 in the Siah2-KD cells resulted in diffuse redistribution of ZO-1 in the cytoplasm, suggesting that ASPP2 is involved in the resistance to TJ disruption, observed upon Siah2-KD (Figure 3f). Indeed, overexpression of ASPP2 attenuated TGF-β mediated TJ disruption, supporting a causative role for ASPP2 in maintaining TJ integrity. Inhibition of Siah2 ligase activity upon ectopic expression of PHYL-130 resulted in increased ASPP2 expression and attenuated TGF-β-mediated TJ dissolution (supplementary Figure S3d and S3d). Collectively, these observations suggest that ASPP2 availability controlled by Siah2 serve to finely tune TJ plasticity. Of interest, comparable expression of N-cadherin upon TGF-β treatment suggests that Siah2-ASPP2 pathway affects cell-cell junction integrity independent of N-cadherin (Figure 3f), consistent with a previous report.[27]

Siah2 regulates 3D morphogenesis of mammary epithelial cells under hypoxia

Given the effect of Siah2 on TJ integrity, which defines the border of apico-basolateral junction, and since ASPP2 is expected to also affect apical polarity, as part of the Par-3 complex,[16, 28] we tested the possible effect of Siah2-ASPP2 module on 3D morphogenesis of mammary epithelial cells. Consistent with a previous report, ∼40% of NMuMG spheres were hollowed after 10 days of organotypic culture (supplementary Figure S4a).[29] Using this model we found that either ASPP2 overexpression or Siah2 KD markedly accelerated the formation of hollowed acini (Figure. 4a). Conversely, the formation of hollowed acini was completely inhibited upon ASPP2 KD (Figure. 4a), pointing to the key role ASPP2 plays in lumen formation. Along the same lines and consistent with Siah2 regulation of ASPP2 within the TJ regulatory complex, KD of ASPP2 in Siah2 KD cells attenuated Siah2 effect on acini formation (Figure 4a). Importantly, impaired lumen formation in ASPP2 KD cells was associated with disruption of apico-basal polarity. Compared with the well-polarized acinar structure, reflected by ZO-1 localization at apical junctions in control cells, ASPP2 KD cells formed solid spheres lacking lumen and apical localization of ZO-1 (Figure. 4b), suggesting that ASPP2 contributes to the formation of polarized structures during 3D morphogenesis. Interestingly, ASPP2 KD also increased acini size, due to increased proliferation index (evidenced by high percentage of Ki-67 positive cells; Figure S4b-d).

Given the roles of Siah2 on cellular adaptation to hypoxia, we set to determine whether the Siah2-ASPP2 regulatory axis affects formation of polarized structure at low oxygen levels. Consistent with earlier reports,[2, 4] Siah2 expression was elevated in cells that were maintained under hypoxia. A corresponding decrease of ASPP2 protein level was observed (Figure 4c and 4d). Notably, Siah2 KD or mutation of Siah2-degron in ASPP2 (ASPP2Mt) attenuated the decrease of ASPP2 protein levels under hypoxia (Figure 4e), thereby suggesting a Siah2-dependent control of ASPP2 stability under hypoxia. Next, we monitored possible changes in early phase of apical polarity formation under normoxia or hypoxia growth conditions. 3D organotypic culture that was maintained for four days under normoxia or hypoxia conditions revealed a significant difference in apical localization of ZO-1 (Supplementary Figure S1e). Interestingly, maintaining 3D cultures under hypoxic conditions for 4 days resulted in a more efficient reduction of apical ZO-1 localization in control (62.3% reduction, $p = 0.03199$), compared with Siah2 KD acini (27.6%, $p = 0.13107$). These observations suggest that reduced formation of apical polarity under hypoxia is Siah2-dependent. Importantly, expression of Siah2-resistant ASPP2 mutant rescued the level of apical ZO-1 localization (50.3%, reduction for control $p = 0.01148$ vs. 21.3% reduction for ASPP2 mutant, $p = 0.15988$) (Figure 4f and 4g), supporting the causal role of Siah2-regulated ASPP2 in apical polarity formation during 3D morphogenesis. Collectively, our findings demonstrate that Siah2 contributes to the control of TJ integrity and epithelial polarity through its regulation of ASPP2 stability, while demonstrating the physiological significance of this regulatory axis under hypoxia. Given that polarity disruption has been implicated in both tumor initiation and progression,[26] and inhibition of Siah2 impairs growth and metastasis in a number of tumor types),[6-9] the Siah2-ASPP2 regulatory axis characterized in this study is expected to play important role in tumorigenesis as in metastasis. Conceptually, the role of Siah2/ASPP2 axis in control of TJ

integrity and tissue polarity under hypoxia, coupled with the established link between hypoxia and EMT, offers a new framework for understanding hypoxia's contribution to tumor metastasis.

Supplementary Material

Refer to Web version on PubMed Central for supplementary material.

Acknowledgments

We thank Laurence M. Brill of the SBMRI Proteomics Facility for mass spectrometric analysis of the Siah2-binding proteins. Support by NCI grants CA111515 and CA128814 (to ZR) is gratefully acknowledged.

References

1. House CM, Moller A, Bowtell DD. Siah proteins: novel drug targets in the Ras and hypoxia pathways. Cancer Res. 2009; 69:8835–8838. [PubMed: 19920190]
2. Nakayama K, Frew IJ, Hagensen M, Skals M, Habelhah H, Bhoumik A, et al. Siah2 regulates stability of prolyl-hydroxylases, controls HIF1alpha abundance, and modulates physiological responses to hypoxia. Cell. 2004; 117:941–952. [PubMed: 15210114]
3. Calzado MA, de la Vega L, Munoz E, Schmitz ML. Autoregulatory control of the p53 response by Siah-1L-mediated HIPK2 degradation. Biol Chem. 2009; 390:1079–1083. [PubMed: 19642869]
4. Kim H, Scimia MC, Wilkinson D, Trelles RD, Wood MR, Bowtell D, et al. Fine-Tuning of Drp1/Fis1 Availability by AKAP121/Siah2 Regulates Mitochondrial Adaptation to Hypoxia. Mol Cell. 2011; 44:532–544. [PubMed: 22099302]
5. Li S, Li Y, Carthew RW, Lai ZC. Photoreceptor cell differentiation requires regulated proteolysis of the transcriptional repressor Tramtrack. Cell. 1997; 90:469–478. [PubMed: 9267027]
6. Schmidt RL, Park CH, Ahmed AU, Gundelach JH, Reed NR, Cheng S, et al. Inhibition of RAS-mediated transformation and tumorigenesis by targeting the downstream E3 ubiquitin ligase seven in absentia homologue. Cancer Res. 2007; 67:11798–11810. [PubMed: 18089810]
7. Ahmed AU, Schmidt RL, Park CH, Reed NR, Hesse SE, Thomas CF, et al. Effect of disrupting seven-in-absentia homolog 2 function on lung cancer cell growth. J Natl Cancer Inst. 2008; 100:1606–1629. [PubMed: 19001609]
8. Qi J, Nakayama K, Gaitonde S, Goydos JS, Krajewski S, Eroshkin A, et al. The ubiquitin ligase Siah2 regulates tumorigenesis and metastasis by HIF-dependent and -independent pathways. Proc Natl Acad Sci U S A. 2008; 105:16713–16718. [PubMed: 18946040]
9. Qi J, Nakayama K, Cardiff RD, Borowsky AD, Kaul K, Williams R, et al. Siah2-dependent concerted activity of HIF and FoxA2 regulates formation of neuroendocrine phenotype and neuroendocrine prostate tumors. Cancer Cell. 2010; 18:23–38. [PubMed: 20609350]
10. Samuels-Lev Y, O'Connor DJ, Bergamaschi D, Trigiante G, Hsieh JK, Zhong S, et al. ASPP proteins specifically stimulate the apoptotic function of p53. Mol Cell. 2001; 8:781–794. [PubMed: 11684014]
11. Vives V, Su J, Zhong S, Ratnayaka I, Slee E, Goldin R, et al. ASPP2 is a haploinsufficient tumor suppressor that cooperates with p53 to suppress tumor growth. Genes Dev. 2006; 20:1262–1267. [PubMed: 16702401]
12. Kampa KM, Acoba JD, Chen D, Gay J, Lee H, Beemer K, et al. Apoptosis-stimulating protein of p53 (ASPP2) heterozygous mice are tumor-prone and have attenuated cellular damage-response thresholds. Proc Natl Acad Sci U S A. 2009; 106:4390–4395. [PubMed: 19251665]
13. Langton PF, Colombani J, Chan EH, Wepf A, Gstaiger M, Tapon N. The dASPP-dRASSF8 complex regulates cell-cell adhesion during Drosophila retinal morphogenesis. Curr Biol. 2009; 19:1969–1978. [PubMed: 19931458]
14. Cong W, Hirose T, Harita Y, Yamashita A, Mizuno K, Hirano H, et al. ASPP2 regulates epithelial cell polarity through the PAR complex. Curr Biol. 2010; 20:1408–1414. [PubMed: 20619648]

15. Sottocornola R, Royer C, Vives V, Tordella L, Zhong S, Wang Y, et al. ASPP2 binds Par-3 and controls the polarity and proliferation of neural progenitors during CNS development. Dev Cell. 2010; 19:126–137. [PubMed: 20619750]
16. Chen D, Padiernos E, Ding F, Lossos IS, Lopez CD. Apoptosis-stimulating protein of p53-2 (ASPP2/53BP2L) is an E2F target gene. Cell Death Differ. 2005; 12:358–368. [PubMed: 15592436]
17. Fogal V, Kartasheva NN, Trigiante G, Llanos S, Yap D, Vousden KH, et al. ASPP1 and ASPP2 are new transcriptional targets of E2F. Cell Death Differ. 2005; 12:369–376. [PubMed: 15731768]
18. Liu ZJ, Lu X, Zhang Y, Zhong S, Gu SZ, Zhang XB, et al. Downregulated mRNA expression of ASPP and the hypermethylation of the 5′-untranslated region in cancer cell lines retaining wild-type p53. FEBS Lett. 2005; 579:1587–1590. [PubMed: 15757645]
19. Zhu Z, Ramos J, Kampa K, Adimoolam S, Sirisawad M, Yu Z, et al. Control of ASPP2/(53BP2L) protein levels by proteasomal degradation modulates p53 apoptotic function. J Biol Chem. 2005; 280:34473–34480. [PubMed: 16091363]
20. Habelhah H, Laine A, Erdjument-Bromage H, Tempst P, Gershwin ME, Bowtell DD, et al. Regulation of 2-oxoglutarate (alpha-ketoglutarate) dehydrogenase stability by the RING finger ubiquitin ligase Siah. J Biol Chem. 2004; 279:53782–53788. [PubMed: 15466852]
21. Szczepanowski M, Adam-Klages S, Kruse ML, Pollmann M, Klapper W, Parwaresch R, et al. Regulation of repp86 stability by human Siah2. Biochem Biophys Res Commun. 2007; 362:485–490. [PubMed: 17716627]
22. Sen N, Hara MR, Kornberg MD, Cascio MB, Bae BI, Shahani N, et al. Nitric oxide-induced nuclear GAPDH activates p300/CBP and mediates apoptosis. Nature cell biology. 2008; 10:866–873. [PubMed: 18552833]
23. House CM, Frew IJ, Huang HL, Wiche G, Traficante N, Nice E, et al. A binding motif for Siah ubiquitin ligase. Proc Natl Acad Sci U S A. 2003; 100:3101–3106. [PubMed: 12626763]
24. Bergamaschi D, Samuels Y, O'Neil NJ, Trigiante G, Crook T, Hsieh JK, et al. iASPP oncoprotein is a key inhibitor of p53 conserved from worm to human. Nat Genet. 2003; 33:162–167. [PubMed: 12524540]
25. Moller A, House CM, Wong CS, Scanlon DB, Liu MC, Ronai Z, et al. Inhibition of Siah ubiquitin ligase function. Oncogene. 2009; 28:289–296. [PubMed: 18850011]
26. Feigin ME, Muthuswamy SK. Polarity proteins regulate mammalian cell-cell junctions and cancer pathogenesis. Curr Opin Cell Biol. 2009; 21:694–700. [PubMed: 19729289]
27. Ozdamar B, Bose R, Barrios-Rodiles M, Wang HR, Zhang Y, Wrana JL. Regulation of the polarity protein Par6 by TGFbeta receptors controls epithelial cell plasticity. Science. 2005; 307:1603–1609. [PubMed: 15761148]
28. Bryant DM, Datta A, Rodriguez-Fraticelli AE, Peranen J, Martin-Belmonte F, Mostov KE. A molecular network for de novo generation of the apical surface and lumen. Nature cell biology. 2010; 12:1035–1045. [PubMed: 20890297]
29. Viloria-Petit AM, David L, Jia JY, Erdemir T, Bane AL, Pinnaduwage D, et al. A role for the TGFbeta-Par6 polarity pathway in breast cancer progression. Proc Natl Acad Sci U S A. 2009; 106:14028–14033. [PubMed: 19667198]
30. Chen M, Gutierrez GJ, Ronai ZA. Ubiquitin-recognition protein Ufd1 couples the endoplasmic reticulum (ER) stress response to cell cycle control. Proc Natl Acad Sci U S A. 2011; 108:9119–9124. [PubMed: 21571647]
31. Debnath J, Muthuswamy SK, Brugge JS. Morphogenesis and oncogenesis of MCF-10A mammary epithelial acini grown in three-dimensional basement membrane cultures. Methods. 2003; 30:256–268. [PubMed: 12798140]

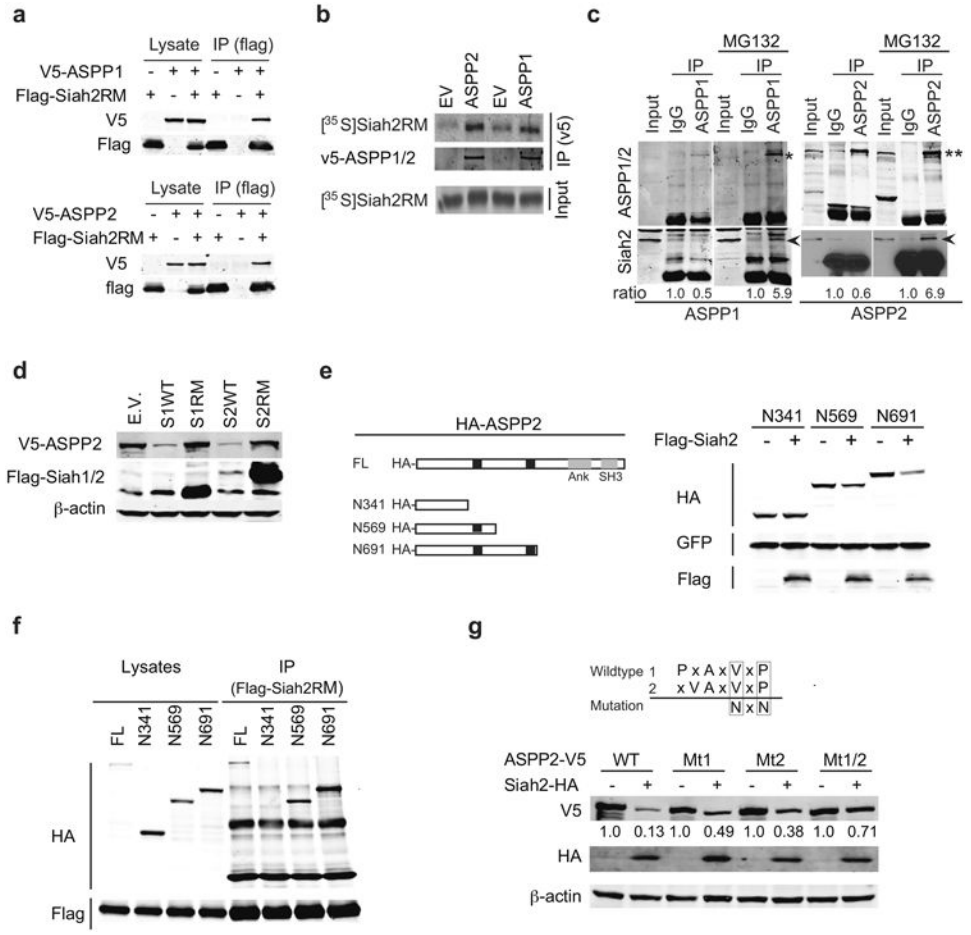

Figure 1.

Siah interacts with- and destabilizes-ASPP1 and ASPP2. (a) Cell Lysates from HEK293T transfected with flag-Siah2 ring mutant (RM), V5-ASPP1 and V5-ASPP2[10] were analyzed by IP (immunoprecipitation) with anti-flag (Sigma, MO, USA) and IB (immunoblot) with anti-V5 (Invitrogen, CA, USA). (b) ASPP1 and ASPP2 immunoprecipitates (IP with anti-v5) and [^{35}S-Met]-labeled Siah2RM were subjected to pull-down analysis, and then to autoradiography. (c) Cell lysates from U2-OS cells cultured in the absence or presence of MG132 (10 μM, 5 h) (EMD Millipore, MA, USA) were subjected to IP with IgG isotype control, ASPP1 or ASPP2 antibodies (Bethyl Laboratories, TX, USA) and IB with anti-Siah2 (Sigma, MO, USA). The single and double asterisks indicate ASPP1 and ASPP2 and arrowheads, Siah2. (d) HEK293T cells were transfected with the indicated plasmids and analyzed by IB. (e) Two black box, indicate two putative Siah degrons; also indicated grey boxes are ankyrin repeats (Ank) and SH3 domains. Cell lysates from HEK293T transfected with indicated constructs were analyzed by IB. (f) HEK293 cells were transfected with the indicated ASPP2 and Flag tagged Siah2RM. Cell lysates were analyzed by IP (flag) and IB (HA). (g) The Siah degrons in ASPP2 were mutated as indicated using site-directed mutagenesis kit (Stratagene, CA, USA). Cell lysates from HEK293T transfected with indicated constructs were analyzed by IB. The relative band intensity was measured by Image J and calculated by setting the band intensity of control lane (without Siah2) as 1.

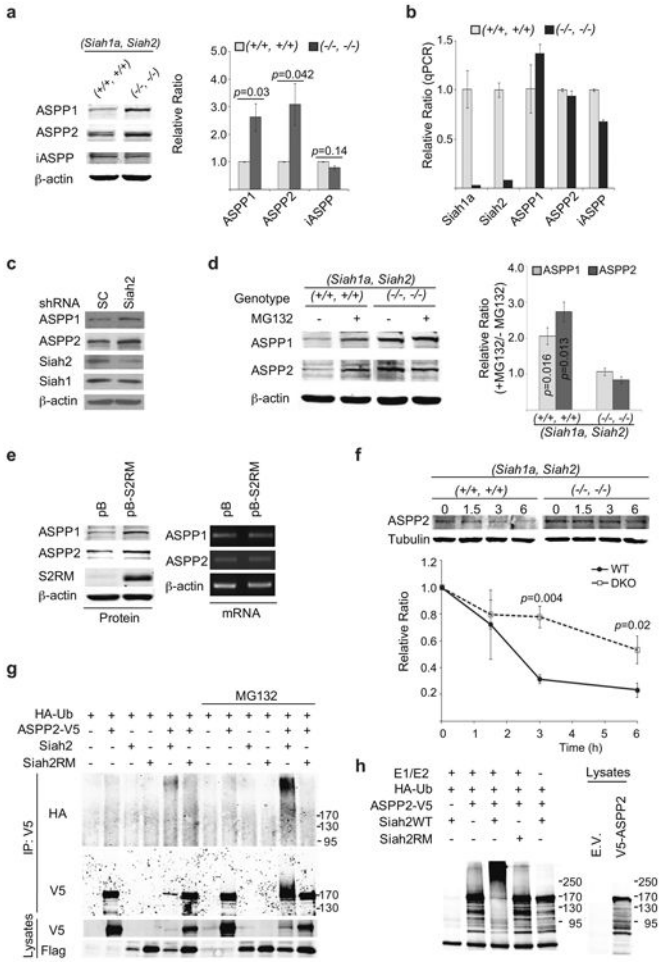

Figure 2.

ASPP1 and ASPP2 are destabilized by Siah-dependent and proteasome-dependent degradation. (a) Lysates of Siah1a^{WT}/Siah2^{WT} (+/+, +/+) or Siah1a^{KO}/Siah2^{KO} (−/−, −/−) MEFs[4] were analyzed with ASPP1, iASPP (Sigma, MO, USA), ASPP2,[11] and β-actin (Santacruz, CA, USA) (left, a representative image). Relative fold increase was analyzed by student *t*-test (*p* values are indicated) from three independent immunoblots (n = 3) (right). (b) Transcript levels were analyzed by qPCR (n = 2). (*ASPP1*; 5′-tgccaaggaacagcgtttaca-3′, 5′-gggcttcaactcgctctttca-3′, *ASPP2;* 5′-caacaaatgctggctactaagga-3′, 5′-cacgagttttccgttgctca-3′, *iASPP2;* 5′-tagaggcccgttttggacg-3′, 5′- cccgatctaggctgctctag-3′, *Siah1a;* 5′-gctgaaaattttgcatatcg-3′, 5′- ccaggaaagttttaggttgg-3′, *Siah2;* 5′-gctgagaactttgcctacag-3′, 5-gctatgcccaaataacttcc-3′, *18s rRNA;* 5′-gtaacccgttgaaccccatt-3′, 5′-ccatccaatcggtagtagcg-3′) (c) Cell lysates from WT MEFs stably expressing scrambled (SC) or *Siah2* shRNA[4] were analyzed by IB with indicated antibodies. Anti-Siah1 was from Sigma (MO, USA). (d) Cell lysates of MEFs cultured in the presence or absence of MG132 (10 μM, 5 h) were analyzed. Fold increase was calculated relative to control (without MG132), and analyzed by student *t*-test (*p* values are indicated) from three independent immunoblots (n = 3) (right). (e) WT MEFs expressing empty vector (pBabe/pB) or pBabe-Siah2RM (pB-S2RM) were analyzed by IB and semi-quantitative PCR. (f) Cell lysates of

MEFs cultured in the presence cycloheximide (50 μg/ml) (EMD Millipore, CA, USA) for the indicated times were analyzed by IB. Relative fold decrease was analyzed by student *t*-test (*p* values are indicated) from three independent immunoblots (n = 3) (lower). Anti-tubulin antibody was from Santa Cruz Biotechnology (CA, USA). (g) Cell lysates from HEK293T cells transfected with the indicated plasmids were subjected to in vivo ubiquitination analysis by IP with anti-V5 and subsequent IB with anti-HA (ubiquitin) antibody.[30] (h) Immunoprecipitated v5-ASPP2 were subjected to an in vitro ubiquitination reaction with recombinant GST-Siah2 WT or RM. Lysates and ubiquitination reaction were analyzed with anti-V5 antibody after extensive washing. All data in graphs are shown as mean ± SD.

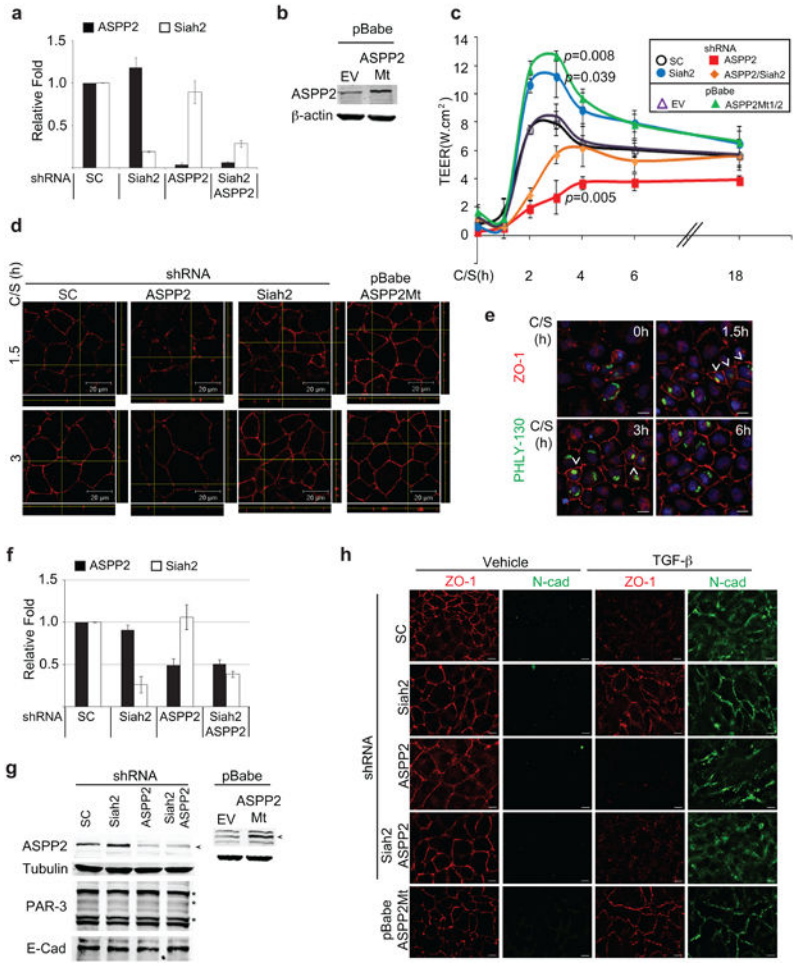

Figure 3.

Siah2 regulates tight junction integrity through ASPP2. (a) Knockdown efficiency of corresponding stable NRK-52E cells was analyzed by qPCR (n = 2). (b) NRK-52E stable cells expressing ASPP2 mutant (ASPP2 Mt) was analyzed. (c, d) NRK-52E cells expressing indicated constructs were depleted of calcium by incubation for 16 h in calcium-free medium (MEM-Eagle Spinner Modification; Sigma, MO, USA) supplemented with 5% dialyzed FBS (GIBCO, CA, USA). Cells were then transferred to calcium-containing DMEM growth medium for the indicated times. (c) Trans-epithelial electrical resistance was assessed at indicated time point. (d) Cells were fixed at indicated time and stained with anti-ZO-1 (Invitrogen, CA, USA). Cells were visualized using confocal microscopy (Zeiss LSM710) with 40×1.2 lens. Corresponding x-z and y-z images were processed using Image J. (e) NRK-52E cells were transfected with HA-PHYL-130 and then subjected to calcium switch assay for indicated time as above. Cells were visualized with anti-HA antibody (Covance, NJ, USA) and anti-ZO-1. The arrowheads indicate the cell border with strong ZO-1 signal. (f) *Siah2* and *ASPP2* transcripts levels were analyzed by QPCR (Roche, IN, USA) of total RNA from NMuMG stable cells expressing corresponding shRNA. Data are presented as mean ± SD (n = 2). (g) Cell lysates from stable NMuMG cells were analyzed with the indicated antibodies; ASPP2, β-tubulin, Par-3 (Millipore, CA, USA) and E-cadherin (BD transduction, CA, USA). The arrowhead indicates ASPP2. The asterisks represent

PAR-3 isoforms. (h) NMuMG stable cells were treated with vehicle (Vech) or TGF-β (5 ng/ml) (R&D systems, MN, USA) for 48 h. ZO-1 (red) and N-cadherin (green) (Santa Cruz Biotechnology, CA, USA) were visualized by immunofluorescent staining. The scale bars, 10 μm.

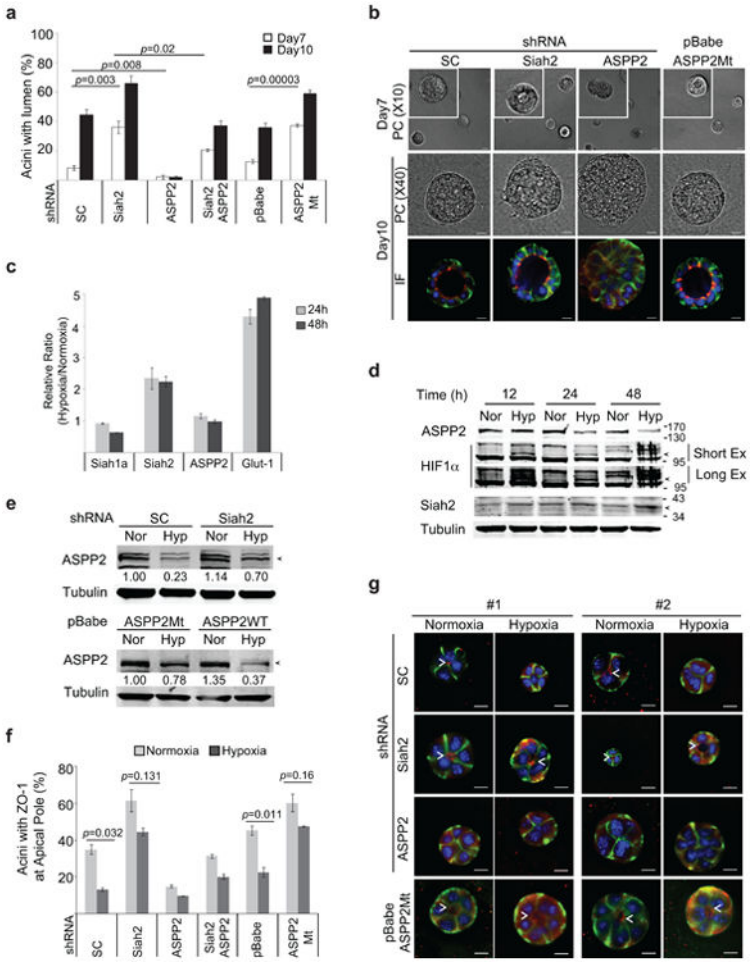

Figure 4.

Siah2 regulates cell polarity in mammary gland epithelial cells. (a) NMuMG cells expressing indicated shRNA(s) were grown in growth factor-reduced Matrigel (BD, CA, USA) using the overlay method as described.[31] Acini with hollowed lumen were counted in a blinded manner at indicated day and the frequency was calculated from total acini (n = 90-140). The data from three independent slides were statistically analyzed (Student *t*-test) and presented as mean ± SD (n=3). (b) Representative images of acinar structures. Scale bars in PC (phase contrast X10) or in PC (X40) indicate 20 or 10 μm, respectively. Acini at day 10 were analyzed using indirect immunofluorescence staining with anti-ZO1 (red) and anti-E-cadherin (green).[31] Nuclear (blue) were visualized by DAPI. (c) The transcripts level in cells grown under normoxia (20% oxygen) or hypoxia (1% oxygen) (Tri-Gas cell culture incubator, Sanyo, Japan) for 24 or 48 h was assessed by qPCR (*Glut1;* 5′-cagttcggctataacactggtg -3′, 5′-gcccccgacagagaagat-3′). The values represent the mean fold-increase under hypoxia. Data are presented as mean ± SD (n = 2). (d) Lysates from NMuMG cells grown under normoxia (Nor) and hypoxia (Hyp) for 12, 24 or 48 h were analyzed by IB. The arrowheads indicate HIF-1α and Siah2. (e) Cell lysates of NMuMG expressing indicated constructs were grown under normoxia or hypoxia for 48h followed immunoblot analysis. Band intensities were normalized to beta tubulin. The arrowhead indicates ASPP2.

(f, g) Cells were grown in Matrigel under indicated oxygen conditions for 4 days. ZO-1 and E-cadherin in acini were visualized using corresponding antibodies. The frequency was calculated from the number of acini with apical localization of ZO-1 counted from total acini (n = 90-120) in a blinded manner. Data from three independent slides are analyzed statistically (Student *t*-test) and presented as mean ± SD (n = 3). (g) Representative images of acinar structures stained with ZO-1 (red) and E-cadherin (green) antibodies. Scale bars, 10 μm. The arrowheads point apical localization of ZO-1.